Critical Magnetic Scattering of Neutrons by Iron

R. D. LOWDE

Atomic Energy Research Establishment, Harwell, England

1. INTRODUCTION

"CRITICAL" phenomena in the magnetic scattering of neutrons were first discovered experimentally in 1953, independently by Palevsky and Hughes[1] and by Squires.[2] A large peak was found at the Curie temperature in the total neutron transmission cross section of polycrystalline iron. In the following year, Shull, Wilkinson,[3] and the author[4] traced this effect to a substantial enhancement of the intensity scattered at crystal settings near to the Bragg condition. During the same period, Van Hove[5] predicted the phenomenon theoretically and gave a neutron cross-section formula based on the Heisenberg conception of a ferromagnet. His ideas are the subject of a number of studies.[6–8]

The theoretical position is examined by Elliott and Marshall in the succeeding paper[9] (hereafter referred to as EM). These authors have given a rather more rigorous discussion of diffraction theory, and have investigated in detail the consequences of assuming certain theoretical models of the scatterer. As Van Hove pointed out, critical scattering is another of the effects whereby neutron diffraction provides a direct check on the applicability of the various theories of magnetism to the substance concerned. In Sec. 4, the evidence about iron is reviewed from this standpoint and it is suggested that the localized-electron type of theory accounts for the phenomena within the limitations of the currently available scattering formulas. If this conclusion is confirmed by further developments of the theory, it will become the third[10] indication from neutron diffraction that the magnetic electrons in iron are sufficiently markedly retained at the atomic sites as to show the properties of a localized-spin wave function.

The following sections give a simple account of the essential phenomena in what is known as the quasi-elastic approximation. Theory and experiment are then compared over a region of the Laue diffraction pattern of an iron crystal covering about 15° of latitude and longitude on either side of the 110 reflection. The "critical" part of the observed counting rates is separated from background and from the intensity scattered by phonons, and its space and temperature dependence studied. Predictions from the Heisenberg theory of ferromagnetism are found to be verified at positions close to the Laue setting, but not at distances in excess of about 10°; it is conjectured that this situation illustrates the conditions of breakdown of the quasielastic approximation. The data analyzed by Gersch, Shull, and Wilkinson (GSW)[11] for scattering at 000 are reassessed in the light of the discussion and shown to be not inconsistent with the conclusions drawn.

This paper is the sixth (VI) of a series[12(a)] to which reference occasionally will have to be made.

2. THEORY

Critical scattering is one of the effects associated with a condensed material in the vicinity of a phase transformation.[12(b)] It may be expected to occur in crystals where there are, under appropriate conditions, atoms of more than one type or existing in more than one state in the lattice. In a system of this kind, for example, a binary alloy, the interactions between like and unlike pairs of atoms will in general be different, and the array will show a certain degree of order, depending on the temperature. The elastic scattering of radiation of propagation vector $\mathbf{k}$ given by such crystals is the sum of the contributions from the various atoms i, of scattering length b_i, at position $\mathbf{R}_i$, with a suitable phase factor; the differential cross section of the assembly is accordingly

$$\partial\sigma/\partial\Omega = |\textstyle\sum_i b_i \exp[i(\mathbf{k}-\mathbf{k}')\cdot\mathbf{R}_i]|^2. \quad (1)$$

For a binary system of components A and B this expression can be manipulated[13] into the form

$$\partial\sigma/\partial\Omega = \tfrac{1}{2}N(b_A-b_B)^2 \sum_{n=1}^{N} \mathcal{P}_{AB}(\mathbf{r}_n) \exp[i(\mathbf{k}-\mathbf{k}')\cdot\mathbf{r}_n] + N\bar{b}^2 \sum_{n=1}^{N} \exp[i(\mathbf{k}-\mathbf{k}')\cdot\mathbf{r}_n], \quad (2)$$

with $\mathbf{r}_n$ a vector connecting lattice sites. Writing χ_A, χ_B for the atomic proportions of the constituents,

$$\mathcal{P}_{AB}(\mathbf{r}_n) = 2\chi_A\chi_B - \mathrm{P}_{AB}(\mathbf{r}_n), \quad (3)$$

[1] H. Palevsky and D. J. Hughes, Phys. Rev. **92**, 202(L) (1953).
[2] G. L. Squires, Proc. Phys. Soc. (London) **A67**, 248 (1954).
[3] M. K. Wilkinson and C. G. Shull, Phys. Rev. **103**, 516 (1956).
[4] Congress of the International Union of Crystallography, Paris (1954).
[5] L. Van Hove, Phys. Rev. **93**, 268; **95**, 249 and 1374 (1954).
[6] A. W. McReynolds and T. Riste, Phys. Rev. **95**, 1161 (1954).
[7] B. Jacrot *et al.* (unpublished).
[8] P. G. de Gennes and A. Herpin, Compt. rend. **243**, 1611 (1957) and unpublished work.
[9] R. J. Elliott and W. Marshall, Revs. Modern Phys. **29**, 75 (1958), following paper.
[10] The other two being the room temperature diffuse reflection[12] and the results of C. G. Shull and M. K. Wilkinson [Phys. Rev. **97**, 304 (1955)] on alloys with certain transition metals.
[11] Gersch, Shull, and Wilkinson, Phys. Rev. **103**, 525 (1956).
[12] (a) Elliott, Lowde, and Marshall, Proc. Roy. Soc. (London) **A221**, 206 (1954); **230**, 46 (1955); **235**, 289 and 305 (1956); and Proc. Phys. Soc. (London) **A69**, 939 (1956). (b) An early discussion of critical scattering was given by L. Landau, Physik Z. Sowjetunion **12**, 124 (1937).
[13] L. Guttman in *Solid State Physics*, edited by F. Seitz and D. Turnbull (Academic Press, Inc., New York, 1956), Vol. 3, p. 156.

and for nonzero $\mathbf{r}_n$ represents the deviation of the pair density function P_{AB} from the value $2x_Ax_B$ that it takes in a random mixture. The first term in (2) is a fourier transform over this function P, and it creates scattered intensity at non-Bragg angles if the degree of order or disorder in the crystal array is imperfect.

In a Heisenberg ferromagnet, the atoms in different states having different neutron scattering lengths are the magnetic atoms with different spin directions. What has been termed critical scattering may most simply be described as the special effects that take place near a phase transformation point, caused by the characteristic behavior of the pair density function of the system under near-critical conditions.

This account is complete for the case of a binary alloy.[13] Applied to a magnetic phase transformation it is equivalent to the quasielastic approximation, according to which the elastic part of the scattering is representative of the whole. Actually the critical magnetic scattering consists of an energy continuum, the inelastic part of which may be attributed to the time dependence of the pair density function. However, because this time dependence has not yet been studied in great detail it is usual at the present day to use the quasielastic approximation. The precise conditions of applicability of this approximation are not known. It is exact at the Curie point, but becomes increasingly untrustworthy as the temperature is varied in either direction, the more so the greater the departure from the Bragg condition. A progressive departure from the simple theory of just this kind has been observed with iron.

Ferromagnetic Critical Scattering

Van Hove has used a spin-spin correlation function of which the time independent part can be written

$$\gamma(R)=\frac{v_0S(S+1)}{4\pi r_1^2R}e^{-\kappa_1R}, \tag{4}$$

with v_0 the volume per spin S. $r_1(T)$ and $\kappa_1^{-1}(T)$ are known as correlation lengths; κ_1 goes to zero at the critical temperature T_c, and thereby creates a maximum in the total scattering. Van Hove derives a critical magnetic differential scattering cross section per atom for a localized-electron ferromagnet of spin S, magnetic form factor f, which in quasi-elastic approximation is

$$\left(\frac{\partial\sigma}{\partial\Omega}\right)(\mathbf{k}')=\sum_\tau(\mathfrak{M}/r_1^2(\kappa_1^2+q^2)). \tag{5}$$

τ is a reciprocal lattice vector. In the high-temperature limit, where interatomic coupling can be ignored, (5) must go over to the paramagnetic cross section

$$\mathfrak{M}=\tfrac{2}{3}S(S+1)\left(\frac{e^2\gamma}{mc^2}\right)^2f^2e^{-2W}, \tag{6}$$

in which e^{-2W} is the Debye factor. $\mathbf{q}=\mathbf{k}-\mathbf{k}'+2\pi\tau$ represents the wave vector of the spin fluctuation which is scattering the neutron, and for a given $\mathbf{k}'$ measures the degree of departure from the Bragg condition. Unlike the propagation vectors appearing in phonon or magnon scattering problems, the $\mathbf{q}$ describing components of the fluctuation in an order-disorder problem are not limited to a single cell of the reciprocal lattice.

One is immediately confronted with the difficulty that expression (5) is $O(1/q^2)$, while the number of terms in the sum increases as q^2. Thus the cross section is apparently infinite. This paradox has been resolved by EM, who show that it springs from the use of (4) at small R, where it is invalid; the contribution of each vector τ can be expressed as the term in (5) plus a second term. Computations from their improved formula Eq. (4.21) demonstrate that in the conditions of the experiment of Sec. 3 the contribution at 110 from all distant reciprocal lattice points except 000 is at most a few percent. Calculations may therefore be made from the 110 term in (5) so long as the existence of this correction is borne in mind.

Laue Diffraction Pattern

A Laue diffraction pattern is formed by allowing white radiation to fall upon the crystal. Suppose that the incident spectrum is $I_0(k)$, with $\int I_0(k)dk=1$; then the critical differential cross section per atom presented to the incident beam is

$$\left(\frac{\partial\sigma}{\partial\Omega}\right)_{\text{Laue}}=\int_0^\infty\frac{\mathfrak{M}I_0(k)dk}{r_1^2(\kappa_1^2+q^2)}. \tag{7}$$

Following a method first given by Van Hove and Riste,[14] this is approximately

$$\left(\frac{\partial\sigma}{\partial\Omega}\right)_{\text{Laue}}(dx,dy)=\frac{\pi I_0(k_L)}{2\sin(\theta_B+\frac{1}{2}dx)}\frac{\mathfrak{M}}{r_1^2(\kappa_1^2+\pi^2\tau^2dx^2+k_L^2dy^2)^{\frac{1}{2}}}; \tag{8}$$

(8) is accurate to a few percent within a few degrees of a typical Laue reflection. dx and dy are angular coordinates of longitude and latitude respectively, relative to the Laue reflection τ considered to be on the equator of the diffraction pattern, θ_B is the grazing angle of incidence onto the planes τ; k_B is the wave vector of neutrons undergoing Laue-Bragg scattering; and $k_L=k_B[1-dx\cdot\operatorname{cosec}(2\theta_B-dx)]$. Equation (8) is the equation of a critical diffuse streak which appears superposed on the streaks due to various other processes such as nuclear and magnetic phonon scattering.

The Space Distribution

According to (8), if dx and dy are sufficiently small so that $k_L\doteqdot k_B$, the critical diffuse intensity should have

[14] Private communication; see also reference 12(b).

contours of equal intensity in the form of ellipses of eccentricity

$$e=k_B/\pi\tau=\operatorname{cosec}\theta_B. \tag{9}$$

At T_c the intensity diffracted into the Laue direction should be exceedingly large, limited only by those crystal imperfections that prevent κ_1 going to zero, and should fall off inversely as the distance measured radially outwards from that position. The transverse half-width of the critical diffuse streak, measured along a line of longitude dx, should be

$$w_h=3^{\frac{1}{2}}\pi dx/k_L. \tag{10}$$

By way of illustration the distribution observed for iron at 110, which will be discussed in Sec. 3, is shown in Fig. 1.

Temperature Dependence

The form of the temperature dependence is most easily understood by considering EM's results for κ_1 and r_1 (their Figs. 1–6). In terms of a reduced temperature $T_r=T/T_c$ one may make the simple approximation

$$r_1^2\doteqdot C/T_r, \quad \kappa_1^2\doteqdot (T_r-1)/C, \tag{11}$$

with $C=0.146a_0^2$ above the Curie temperature; whence from (8)

$$\left(\frac{\partial\sigma}{\partial\Omega}\right)_{\text{Laue}} \sim \frac{T_r}{[T_r-1+(C\pi^2\tau^2dx^2+Ck_L^2dy^2)]^{\frac{1}{2}}}. \tag{12}$$

For small dx, dy the quantity (12) has a sharp maximum at T_c; but with increasing departure from the Laue setting the maximum is reduced, and eventually disappears at $q=1/(2C)^{\frac{1}{2}}$. At positions still farther removed from the Bragg condition the expression (12) rises monotonically through the Curie point and $\partial\sigma/\partial\Omega$ continues to increase towards the paramagnetic cross section asymptotically. From Eq. (8), at small dx, dy the influence of κ_1 is dominant; this fact is the cause of the maximum. At more distant settings the effect of κ_1 tends to be suppressed, and the cross section becomes inversely proportional to r_1^2.

This behavior is illustrated by the curves of Fig. 2,

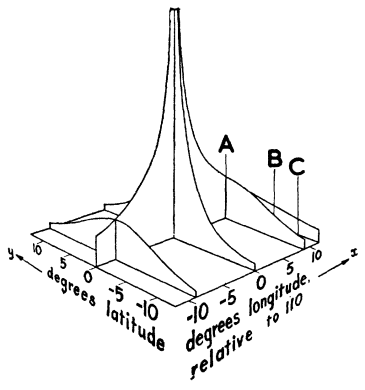

FIG. 1. The observed distribution around 110 in the Laue pattern of the "critical" component of neutron scattering from iron at the Curie temperature. $\theta_B=20°$.

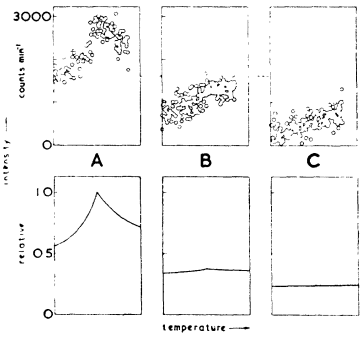

FIG. 2. Observed and calculated temperature dependence of the critical magnetic scattering at A, B, and C of Fig. 1. For each frame the temperature is plotted along a horizontal scale which runs from $T_c-100°$K to $T_c+100°$K. At A the dominant effect is the temperature variation of κ_1; at C it is the variation of r_1. The progressive loss of agreement with theory from A to C may be the result of breakdown in the quasielastic approximation. A broken line between frames of the upper series shows the level of scattering to be expected in the high-temperature limit from an idealized paramagnet with $S=1$.

which were computed directly[15] from Eq. (7) for the experimental conditions of three sets of readings discussed in Sec. 3, using the κ_1 and r_1 of a Heisenberg ferromagnet. The three minimum values of q^2 for the cases A, B, and C were, respectively, 0.0596, 0.344, and 0.70.

A Complication

Computation from Eqs. (4.21) of EM has brought to light the unexpected complication that, even at the scattering angles of ~50° used in the present experiment, there is an appreciable contribution from critical "small-angle scattering"—i.e., scattering caused by the region of reciprocal space near 000 of the very long wavelengths present in the incident beam. The wavelengths concerned are principally between about 3 and 12 A. On paper, this effect should account for some 10% of the intensity at A of Fig. 2, from which the results for κ_1 are deduced. In practice the longer wavelengths do not reach the counter, on account of the enormous absorption to which they are subject, and the correction is again only a few percent. It is, however, comparatively difficult to estimate, and adds to the error in determining r_1. The results for κ_1 are estimated to be unaffected within the limits of the statistical uncertainty.

3. EXPERIMENT

Surveys of the neutron scattering have been made in the neighborhood of the Laue reflection 110 with $\theta_B=20°$, covering that portion of the diffraction pattern whose appearance at room temperature is illustrated in Fig. 3 of Paper IV. The room temperature pattern consists of a clearly defined diffuse streak along the equator, standing out above a virtually flat background. This diffuse streak is the result of one-quantum scatter-

[15] To compute counting rates from the right-hand side of Eq. (7), $I_0(k)$ must be multiplied by the counter efficiency $\epsilon(k)$.

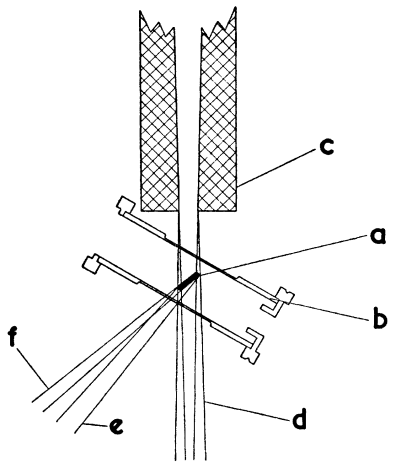

FIG. 3. Arrangement of spectrometer parts within the thermal insulation of the furnace. a—the crystal; b—a 1-in. diam. mullite bobbin directing hot argon over the crystal; c—a B_4C collimator; d—the incident neutron beam; e—the Laue reflection 110; f—radiation scattered at +9° from 110.

ing by phonons and magnons; any study of critical scattering at nonzero *hkl* must involve some procedure for separating off the contributions from such processes.

Apparatus

An iron crystal, consisting of a trapezoidal slab of mean dimensions 2.3×12.6×9.3 mm³, was taken from the batch whose analysis was given in Paper IV and mounted with the [$\bar{1}$, 1, 0.82] axis vertical. As illustrated in Fig. 3, the cut was so arranged as to provide a maximum degree of focusing for the scattering angle 49° at which the results of Fig. 2 were taken. The crystal was attached by a mixture of two alumina cements to an alumina cradle held in a pyrophilite boat, and the whole assembly mounted in a 1-in. diam. mullite bobbin of wall thickness 1 mm. Argon was continuously recycled over a 1-kw electric heater and through the bobbin, where a pyrophilite nozzle, not shown in the figure, directed hot gas onto the crystal at a flow rate of ~25 l min^{-1}. Conical collimators of apex angle $2\frac{3}{4}°$ defined an incident beam of predominantly Maxwell neutrons from a source at 40°C within the reflector of BEPO. The last collimating section, within the furnace lagging, was made of sintered B_4C. A 1-in. diam BF_3 counter at a radial distance of 17 in. functioned as the detector. Both the collimation and the entrance window of the counter shield were chosen to simulate exactly the geometry used in the room-temperature experiment of Paper IV.

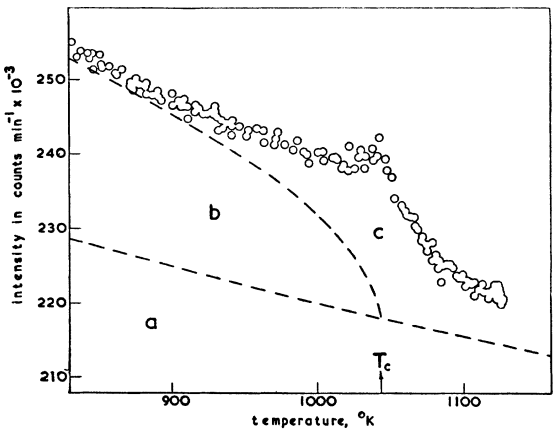

FIG. 4. Critical scattering from the 110 planes of an iron crystal observed at the Laue reflection angle with $\theta_B = 20°$. The broken lines give a schematic decomposition of the intensity into a—nuclear Bragg reflection, b—magnetic Bragg reflection, and c—critical scattering.

Critical Scattering under the Bragg Condition

The remarkable scale of spin-fluctuation effects is demonstrated by the intensity recorded at the Laue position, shown as a function of temperature in Fig. 4.

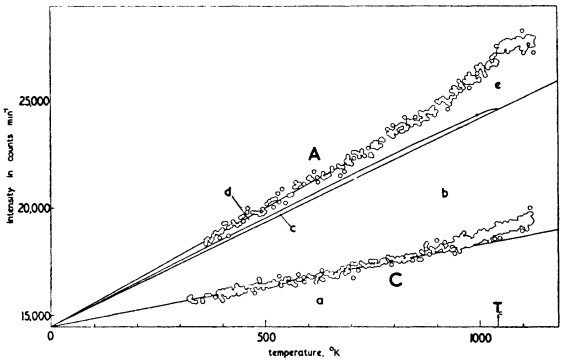

FIG. 5. Intensities recorded at: A—an equatorial position in the 110 diffuse intensity, +9° from the Laue reflection; and C—a position in the background at the same longitude, but at latitude 12°. Inelastic neutron scattering in the mullite furnace walls gives rise to the essentially linear background, a. Above this, the intensity at A consists of, b, nuclear phonon scattering, which has been extrapolated linearly; c, magnetovibrational scattering; d, magnon scattering; and, e, critical scattering.

Even with $2\frac{3}{4}°$ collimation, the peak of the critical component rises to a magnitude comparable with the intensity associated with magnetic Bragg reflection at low temperatures. Owing to the heavy extinction suffered by a Laue reflection in a crystal of this size it is difficult to give an accurate breakdown of the counting rate into its components; an approximate resolution has been indicated on the diagram.

Background, and Isolation of the Critical Phenomenon

Neutrons scattered from the mullite bobbin provided a background count roughly equal in magnitude to the phonon diffuse intensity. Figure 5 reproduces curves of the counting rate against temperature for two detector settings—*A* of Paper IV, Fig. 3, and a position in the background region which is labeled *C* in Fig. 1. The latter curve shows that within the limits of statistical

error the background is linear with temperature at least up to 750°K. At higher temperatures, critical effects become apparent at these positions. They have been isolated from background by means of a straight-line extrapolation such as that shown at Fig. 5C, and the nonlinear part has been assumed to be the critical fraction.

Curve A of Fig. 5 records the intensity at a point in the middle of the diffuse streak, and its linear portion therefore falls above C by the amount of the phonon and magnon scattering at the equator. It is known from the studies of Paper IV that this intensity, in the given geometry and with $\langle(\mathbf{e}\cdot\boldsymbol{\kappa})^2\rangle_{Av}=\frac{1}{3}$, is 88% phonon scattering. Assuming that this phonon component is linear over the whole temperature range, which should be true within 2%, a breakdown of the total scattering at A can therefore be made in the manner illustrated.

Comparison with Eqs. (7)–(10)

The Space Distribution

Figure 6(a) presents a series of surveys at different temperatures, taken across the direction of the diffuse streak along the line of longitude +9°. They have the character of the transverse contours in Fig. 3 of Paper IV, except that the background has been subtracted.

The central hump whose shape appears on all curves is the same essentially one-quantum inelastic scattering which appeared at b, c, and d in Fig. 5. However, with increase of temperature above about $\frac{2}{3}T_c$, conspicuous wings are seen to spread out progressively from the sides of the hump, in such a way that the central peak is raised up and reaches a maximum height at T_c. This phenomenon strongly suggests that some special scattering process is present, superposing its distribution on that of the processes creating the hump. If the appropriate nuclear phonon intensity from Fig. 5 is subtracted from the peak at T_c, the point O in Fig. 6(b) is obtained. A hatched area in this diagram gives the shape of the critical distribution predicted by Eq. (8). This equation, fitted at the center, accounts for the magnitude of the wings.

By means of the extrapolation procedures of Fig. 5, the critical intensity has been isolated at twelve points in the neighborhood of 110, and a picture of its distribution at T_c appears in Fig. 1. The general predictions of Sec. 2 are recognizably brought out. A surface is indicated having level contours which are roughly elliptical; the eccentricity of the contour through longitude +9°, latitude +0° is 2.4, which may be compared with 2.9 calculated from the approximate formula (9). The section along the line of longitude +9° has a half-width at half-height of 8°, as against 7° given by (10).

Temperature Dependence

Counting rates at A, B, and C are shown as a function of temperature in the upper part of Fig. 2. The simple prediction $q\doteqdot 1/(2C)^{\frac{1}{2}}$ of Sec. 2 would suggest that the maximum should be lost at about the position B, and

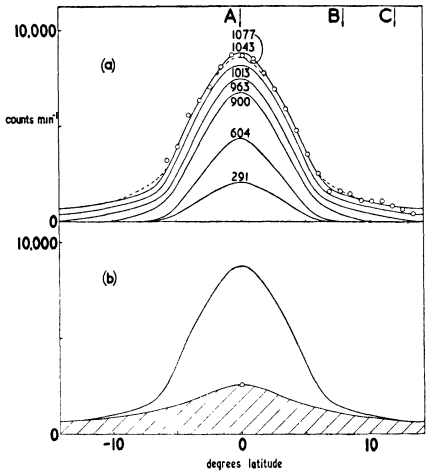

FIG. 6. (a). Transverse surveys of the diffuse intensity along the line of longitude +9° containing A, B, and C in Fig. 1, taken at various temperatures marked in °K. Points for the topmost curve indicate the accuracy of measurement. Up to 700°K, a characteristic hump is found, increasing in proportion to the temperature, and due to one-quantum inelastic processes. At temperatures beyond $\frac{2}{3}T_c$ another type of scattering appears to be superposed on this distribution. (b). A resolution of the contour at T_c into phonon and critical magnetic parts. The hatched area is computed from Eq. (8).

this indeed occurs. For the three cases shown, the angle[16] between $\mathbf{k}-\mathbf{k}'$ and τ takes the values 4° 30′, 10° 53′, and 15° 34′. Agreement with EM is excellent in the first case, but deteriorates with increasing departure from the Bragg setting and is only qualitative at C.

As shown in Sec. 2, the results at A are strongly dependent on κ_1; they will be used to derive that function in the next section. By the same argument, the intensity at C is supposed to be nearly proportional to r_1^{-2}, the influence of κ_1 being reduced to a small correction. However, there is patent disagreement with theory at C. It follows that either the basic physical assumptions of EM are inapplicable to iron, or that the approximations have in some way broken down. Since the calculations appear to fit the case of A, a possible explanation is that the time-dependent parts of the pair density function have begun to exert an appreciable effect at C, thus invalidating Eq. (7) at this setting. If, nevertheless, Eq. (7) be applied to illustrate the magnitude of the discrepancy, an effective $r_1(T)$ is deduced which is in violent conflict with EM. For example, an analysis of the points above T_c in Fig. 2C led to a temperature dependence having the approximate form $r_1\sim T_r^{-3.3\pm0.5}$ over the range concerned. Within the observational error this is the same dependence as that derived by GSW,[11] also on the basis of a quasielastic theory.

4. DISCUSSION

It will have become evident that a scattering process closely similar to that predicted by Landau and Van

[16] These angles effectively represent the degree of departure from the Bragg condition. They have the same significance as the scattering angle in Shull's work,[3,11] and may be directly compared after multiplication by a factor ~0.55 which takes into account the difference in crystallographic arrangement.

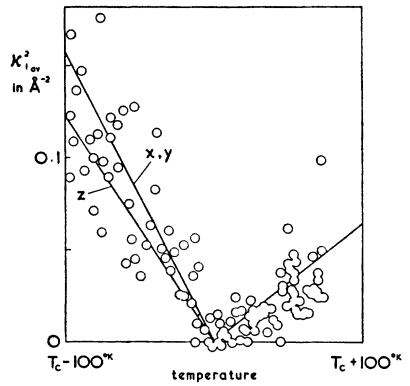

FIG. 7. Absolute values of $\langle\kappa_1^2\rangle_{Av}$, derived from the experimental points of Fig. 2A by use of Elliott and Marshall's theoretical $r_1(T)$. Solid lines show the theoretical κ_1^2 for a body-centered cubic Heisenberg ferromagnet with $S=1$ above and $S=\frac{1}{2}$ below the Curie temperature.

Hove takes place in the neutron diffraction by iron at 110. At $\kappa_1=0$, with $r_1=$constant, the influence of the factor q^2 in (5) is demonstrated in Fig. 1; while at large and small q, respectively, the temperature dependence of both the amplitude and range of the spin-spin correlation, qualitatively determined by the thermodynamic restrictions on r_1 and κ_1, is directly apparent from the behavior of the cross section in Fig. 2. When a future theory becomes available, taking proper account of the time-dependent effects, κ_1 and r_1 can be deduced unambiguously from these figures. The present indications are that the quasielastic approximation is an insufficiently powerful tool for this purpose. It is interesting to enquire whether the current state of theory and experiment does nevertheless bear on the question of what wave functions should be used to describe the magnetic electrons in iron.

At the time of this Conference, the only theoretical analysis which has been pursued to the extent required for a detailed comparison with experiment is EM's study of a body-centered cubic Heisenberg ferromagnet with $S=1$ above the Curie temperature and $S=\frac{1}{2}$ below, the critical scattering being calculable in quasielastic approximation only. Now there is reason to believe that the major effect of the time-dependent correlations on the theory will be to multiply (5) by a scaling factor. Since r_1 itself enters (5) as a scaling factor, and since the influence of r_1 becomes dominant only far from the Bragg condition where the quasielastic approximation becomes unreliable, it would follow that a determination of $r_1(T)$ from (5) must be viewed with some reservation. In Fig. 2C, indeed, from which $r_1(T)$ would normally be derived, the theoretical prediction is manifestly unsound in that it shows no sign of allowing for the observed drop in the cross section to virtually zero as the temperature is lowered to $\frac{2}{3}T_c$. GSW's determination likewise depends strongly on measurements at roughly about the same values[16] of q, and it is possible that their method is subject to the same error. The disagreement with EM's temperature dependence for r_1 is therefore not necessarily significant, and judgment must be suspended until a more profound analysis is available.

Quantities which can be compared with theory at the present time are $r_1(T_c)$, the value at the temperature for which the quasielastic approximation is exact, and $\kappa_1(T)$, deduced on certain assumptions from Fig. 2A. The $r_1(T_c)$ obtained with polycrystalline iron by GSW is 1.12 ± 0.05 A, in absolute agreement with EM. In the present experiment the heavy extinction in the Laue reflections makes it necessary to calibrate the intensities by applying phonon scattering theory to the unhatched area in Fig. 6(b); when this is done, and Eq. (7) applied to Fig. 2, a figure of $r_1(T_c)=1.4$ A is found. The discrepancy between this figure and GSW's is presumably attributable to the highly indirect nature of this latter calibration.

Turning to the evidence about κ_1, it is consistent to deduce from Fig. 2 that the theory is sound over that range wherein κ_1 dominates the temperature dependence. $\kappa_1(T)$ is determined absolute from the *shape* of the intensity curves. It has been derived from Fig. 2A by the following procedure: the experimental counting rates of Fig. 2A were multiplied by the *theoretical* $\langle r_1^2\rangle_{Av}$ averaged over the three axes of the crystal, and compared on a relative scale with a fully theoretical computation giving[15] $\int[f^2e^{-2W}\epsilon I_0(k)dk/(\kappa_1^2+q^2)]$ (also averaged over the three axes) as a function of κ_1^2. The procedure used for averaging over x, y, and z does not introduce a significant error. Figure 7, which gives the result, expresses the agreement with EM in a rather more fundamental manner from Fig. 2A.

Support for this appraisal of the position is provided by the GSW data on κ_1 above the Curie temperature. If $\kappa_1^2(T)$ is reevaluated at 000 on the basis solely of data taken at 0.9° of scattering angle,[17] and using again the theoretical r_1^2, an approximate straight line is obtained which is in roughly the same degree of agreement with EM as the points of Fig. 7.

A tentative case for the Heisenberg theory of ferromagnetism in hot iron might therefore be rested on the following argument: that r_1 is correctly predicted at the Curie temperature; that the critical scattering covering several degrees of angle around two reciprocal lattice points is explained over a range of ±100°K; and that the evidence suggests that this reasonably exhausts the scope of the available approximations. On the other hand, a strict demonstration that the quasielastic approximation was valid over the appropriate range of the parameters would bring the Heisenberg theory into direct conflict with experiment.

ACKNOWLEDGMENTS

I am much indebted to Professor L. Van Hove for a valuable discussion of his theory. Special thanks are also due Dr. R. J. Elliott, Dr. L. Guttman, and Dr. W. Marshall for extremely helpful conversations. The practical cooperation of D. N. Wilson and D. A. Wheeler is acknowledged gratefully.

[17] A procedure which is greatly facilitated by referring to Oak Ridge National Laboratory, Report No. 1975, (1955), pp. 54–55.